J Solid State Electrochem (2000) 4: 298–303

ORIGINAL PAPER

C.U. Ferreira · Y. Gushikem · L.T. Kubota

Electrochemical properties of Meldola's Blue immobilized on silica-titania phosphate prepared by the sol-gel method

Received: 22 June 1999 / Accepted: 7 September 1999

Abstract The mixed oxide phosphate $(\equiv SiO)_2Ti(O_3POH)_2$ having a specific surface area of $S_{BET} = 595\ m^2\ g^{-1}$ and an average pore volume of 0.43 mL g^{-1} was prepared by the sol-gel processing method. The material showed the following characteristics: Ti = 11.6 wt% and P = 10.5 wt%; ion exchange capacity of 0.60 mmol g^{-1}. Meldola's Blue (MLB) dye was adsorbed, by an ion exchange reaction, from an aqueous solution in a quantity of 0.62 mmol g^{-1}. The dye was strongly retained and was not easily leached from the matrix even in presence of 0.5 M electrolyte solution. Changing the solution pH between 2.5 and 7.0, the midpoint potential of the dye-adsorbed $(\equiv SiO)_2Ti(O_3POMLB)_2$ matrix carbon paste electrode remained practically constant, i.e. about 20 mV vs. SCE. This is not the usual behaviour of MLB since its midpoint potential changes considerably in solution phase as the pH is changed. The modified electrode has proved to be stable and electrocatalytically active for hydrazine oxidation at pH 6.

Key words Silica-titania phosphate · Sol-gel processing · Meldola's Blue · Carbon paste electrode · Hydrazine electrooxidation

Introduction

Metal oxides grafted on to silica-gel surfaces have been used as electron mediator immobilization matrices to develop a new class of electrodes [1–8]. More recently, binary oxides of the type SiO_2/M_xO_y prepared by the sol-gel processing method have also been applied for such a purpose [9–15]. Gels or xerogels prepared by this method are considered as new materials for electrode modifications as they display large surface areas and offer a possibility of reacting with a Brønsted acid, resulting in a highly dispersed immobilized acid [16]. Of particular interest is the SiO_2/TiO_2 binary oxide, prepared by the sol-gel processing method, when allowed to react with phosphoric acid. The resulting material, SiO_2/TiO_2/phosphate, containing the immobilized HPO_4^{2-} species, shows a large ion exchange capacity [17].

Meldola's Blue redox dye has been used to prepare modified electrodes and it has been successfully used as an amperometric sensor for β D-glucose and NADH determinations [18, 20–22]. Recently, Nile Blue and Methylene Blue dyes were immobilized by means of an ion exchange reaction in bulk zirconium phosphate and the resulting material was used to prepare a carbon paste electrode for electrocatalytc oxidation of NADH and ascorbic acid [23, 24]. Since the bulk phase zirconium phosphate is obtained as a fine powder with no mechanical resistance and has a small specific surface area, an attractive alternative is to immobilize the dye in the sol-gel prepared SiO_2/TiO_2/phosphate matrix, where the Brønsted acid character is similar to that shown by the bulk titanium phosphate phase. Using this procedure may result in a material having an additional advantage such as improved mechanical and thermal stability and presenting also a higher specific surface area. In order to test the potential of this material as a substrate for developing a new class of electrode, Meldolas's Blue was immobilized on SiO_2/TiO_2/phosphate and the carbon paste electrode of this material was used to study the hydrazine electrocatalytic oxidation. The hydrazine molecule has a relatively high formal oxidation potential, i.e. 0.92 V vs. SCE using a conventional electrode [25], so the use of chemically modified electrodes in order to minimize this effect appears to be very desirable. An additional advantage in using porous materials is that the dispersion of electroactive species on the surface of such kinds of materials has resulted in a great improvement in stability and catalytic action [16].

C.U. Ferreira · Y. Gushikem (✉) · L.T. Kubota
Instituto de Química, UNICAMP, C.P. 6154,
13083-970 Campinas, S.P., Brazil

Experimental

Preparation

The SiO_2/TiO_2 binary oxide matrix was prepared by mixing 17.6 mL of tetraethyl orthosilicate (Aldrich) and 1.7 mL of 1.3 M HNO_3 and the solution refluxed for 2.5 h at 353 K. About 70 mL of dry ethanol and 3 mL of tetrabutyl orthotitanate (Fluka) was added and the mixture was stirred for 2 h at room temperature. Then, 9.5 mL of a 1 M HNO_3 aqueous solution was slowly added to the reaction medium and stirred for more 2 h at room temperature. The resulting xerogel was dried in an oven for 30 h at 323 K and the solid ground in a mortar and sieved to a particle size of about 0.25 mm. The gel was obtained by heating the xerogel at 773 K under an air flux for 24 h.

The incorporation of phosphate into the matrix was made by immersing 4 g of SiO_2/TiO_2 in 60 mL of 0.2 M H_3PO_4 solution and the mixture stirred during 4 h at 298 K. The solid was filtered, washed with water, and dried for 1 h at 353 K in an oven. Chemical analysis of the SiO_2/TiO_2/phosphate sample was made by slowly adding hydrofluoric acid (40 wt% solution) until complete dissolution of the solid, the resulting solution was diluted with 100 mL of water and then concentrated NH_4OH was added until precipitation of the hydrous titanium oxide occurred. The solid was allowed to stand for 3 h, filtered, washed with water, calcined at 1073 K, and weighed as TiO_2. The filtered solution was acidified with sulfuric acid, and the amount of phosphorus was determined spectrophotometrically using the molybdenum Blue method.

The specific surface area was determined by the BET multipoint method on a Micromeritcs Flow Sorb II 2300 apparatus connected to a flow controller. The average pore volume of the samples was determined by the mercury intrusion technique on a Micromeritcs Pore Size 9320 apparatus.

The scanning electron microscopy images of the samples were obtained by dispersing the solid on a double-face conducting tape and fixed on a brass support. Coating of the particles with graphite was made by the deposition technique using a sputter low-voltage LVC 76 apparatus from Plasma Science. The microscope used was a JEOL JSM T-300 connected to a secondary electron detector and to an X-ray dispersive energy analyser from Northem.

The ^{31}P NMR spectrum was obtained by the cross-polarizing magic angle spinning technique. The sequential pulse conditions used were a contact time of 1 ms, with 2 s intervals between the pulses, and an acquisition time of 11 ms. Phosphoric acid (85 wt%) was used as reference. The equipment used was a Brucker AC 300P spectrometer operating at 121 MHz.

The ion exchange capacity of the sample was determined by immersing 100 mg of SiO_2/TiO_2/phosphate in 50 mL of 0.5 M NaCl solution and the mixture shaken for 8 h. The released H^+ from the exchange reaction was titrated with 0.05 M NaOH standard solution.

Meldola's Blue (MLB) was adsorbed on the SiO_2/TiO_2/phosphate by immersing 2 g of the sample in 10 mL of an aqueous solution of 1% (m/v) MLB. The mixture was shaken for 24 h and the solid was filtered, washed with water, and dried for 30 min at 393 K in an oven. From the C, H, N elemental analysis, the quantity of the adsorbed MLB was determined.

The carbon paste electrode was prepared by mixing 30 mg of SiO_2/TiO_2/phosphate with 30 mg of graphite (Fluka) and a drop of liquid paraffin. This paste was deposited into a cavity in contact will a platinum disk fused at the end of a glass tube with 3 mm internal diameter.

Electrochemical measurements

The electrochemical studies were made by using the cyclic voltammetry technique and a three-electrode system, where a carbon paste of the material, a saturated calomel electrode (SCE), and a platinum wire were used as working, reference, and counter electrodes, respectively. All the measurements were carried out under pure argon atmosphere. The equipment used was the PAR EG&G model 273A galvanostat-potentiostat.

Electrocatalytic oxidation of hydrazine was studied by successive addition of 50 μL aliquots of 0.01 M hydrazine sulfate solution into a electrochemical cell containing 10 mL of 0.5 M KCl solution at pH 6.0.

Results and discussion

Characteristics of the material

The SiO_2/TiO_2/phosphate material presented a specific surface area $S_{BET} = 595\ m^2\ g^{-1}$ and an average pore volume of 0.43 mL g^{-1}. Chemical analysis of the material showed the following results: Ti = 11.6 wt% and P = 10.5 wt%. The ion exchange capacity was 0.60 mmol g^{-1} and the amount of adsorbed MLB, determined by elemental analysis, was 0.62 mmol g^{-1}. Assuming that the adsorbed phosphate is the HPO_4^{2-} species (see discussion below), we conclude that only a fraction of the protons were exchanged (estimated exchange capacity is 3.4×10^{-3} mol g^{-1}).

Figure 1 shows the scanning electron microscopy and the respective EDS images of the SiO_2/TiO_2/phosphate

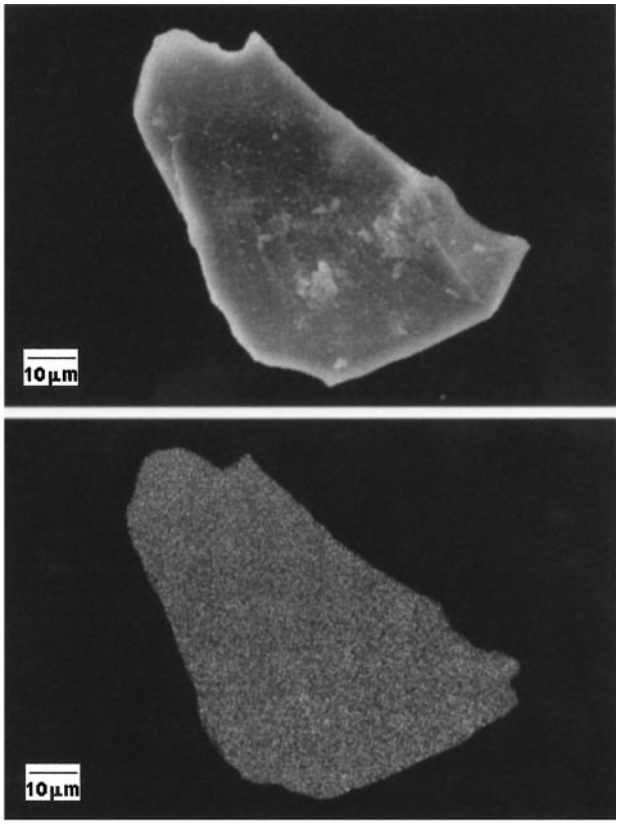

Fig. 1 Scanning electron microscopy image of **a** $(\equiv SiO)_2Ti(O_3POH)_2$ and **b** the corresponding EDS images of titanium

material. In Fig. 1a there is no evidence, within the magnification used, of phase separation of each component. The bright points in Fig. 1b are due to the titanium atom fluorescence emission line Ti (kα) = 4.51 keV [26]. The EDS images indicate that titanium atoms are highly dispersed in the silica matrix with no detectable oxide particle agglomerates.

The ^{31}P NMR spectrum presented only one peak at −10 ppm due to the HPO_4^{2-} species in the matrix [17]. For bulk $Ti(HPO_2)_2 \cdot 2H_2O$ the ^{31}P NMR peak is found at −9.3 ppm [27]. Therefore, formally we can represent the material as $(\equiv SiO)_2Ti(O_3POH)_2$. The incorporation of MLB in the $(\equiv SiO)_2Ti(O_3POH)_2$ matrix can be represented by the following ion exchange reaction:

$$(\equiv SiO)_2Ti(O_3POH)_{2(s)} + 2MLB^+_{(sln)} \rightleftharpoons (\equiv SiO)_2Ti(O_3POMLB)_{2(s)} + 2H^+_{(sln)} \quad (1)$$

where s and sln refer to solid and solution phase, respectively, and MLB^+ to the form I of the dye in the solution phase (see Scheme 1). It should be remembered that only about 20% of the protons were exchanged.

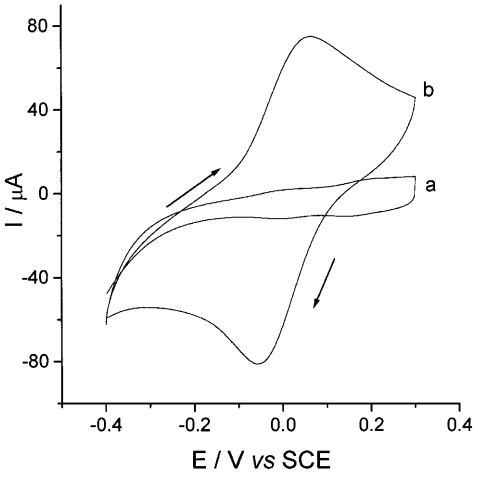

Fig. 2 Cyclic voltammetry curves for *a* $(\equiv SiO)_2Ti(O_3POH)_2$ and *b* $(\equiv SiO)_2Ti(O_3POMLB)_2$. Scan rate 20 mV s^{-1}; 0.5 M KCl solution; pH 6.5

cathodic (were I is the variation of the peak current intensities and I_0 is the initial peak current intensity),

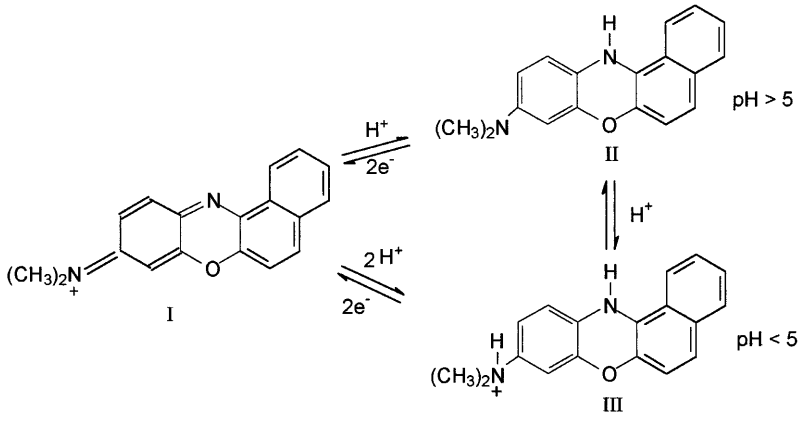

Cyclic voltammetry studies

Figure 2 shows the $(\equiv SiO)_2Ti(O_3POH)_2$ and $(\equiv SiO)_2Ti(O_3POMLB)_2$ cyclic voltammetry curves, both obtained under the same conditions, i.e. 0.5 M KCl supporting electrolyte solution at pH 6.5 and a scan rate of 20 mV s^{-1}. In Fig. 2a, no peak currents are observed for $(\equiv SiO)_2Ti(O_3POH)_2$. A peak current with a midpoint potential of $E_m = 20$ mV [$E_m = (E_{pc} + E_{pa})/2$, where E_{pa} and E_{pc} are the anodic and cathodic peak potentials, respectively] is observed for $(\equiv SiO)_2Ti(O_3POMLB)_2$ (Fig. 2b). This value is shifted towards more positive potentials when compared to those observed for soluble species (−180 mV), suggesting stabilization of the reduced form.

In order to know how strong is the dye adsorbed on the matrix, a test consisting of cycling the potential many times between −0.4 and 0.4 V with the electrode of the material immersed in 0.5 M KCl solution was made. The I/I_0 plot for both peak currents, anodic and show that the percentage variation after 150 cycles is relatively small, i.e. about 25%. The immobilized dye shows a small tendency of leaching off from the substrate surface by the supporting electrolyte solution, indicating its great affinity for the solid exchanger phase.

Study of the solution pH on the electrode response

It has been previously reported that the MLB midpoint potential is strongly dependent on the solution pH. It presents, according to the solution pH, different protonated species (see Scheme 1), which affect the midpoint potential of the redox process [18]. When adsorbed on a graphite surface, MLB gives $pK_a = 5$ and thus at pH < 5 form III will predominate while at pH > 5 form II will predominate. No pK_a value for MLB in the solution phase is available but it is supposed to be close to similar phenoxazine dyes, i.e. $pK_a = 4$–5 [19].

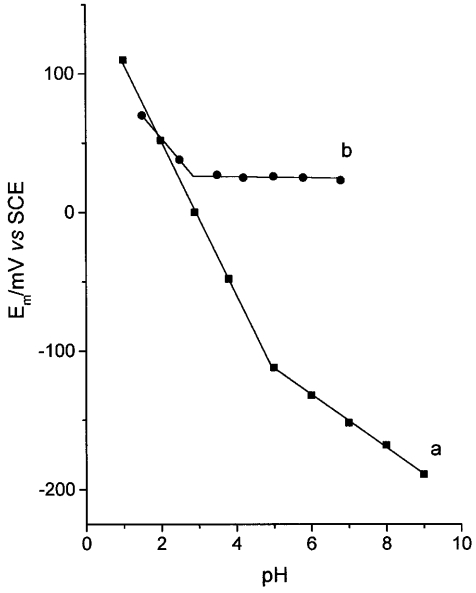

Fig. 3 Change of the midpoint potentials, E_m, of the adsorbed MLB with the solution pH: *a* graphite/MLB; *b* $(\equiv 0SiO)_2Ti(O_3POMLB)_2$

Figure 3a shows that for MLB adsorbed on a graphite-modified electrode surface, between pH 1 and 7, E_m varied between −200 mV and 120 mV [18]. For the $(\equiv SiO)_2Ti(O_3POMLB)_2$ electrode, in the pH range between 2.5 and 7 the potential change was very small (Fig. 3b), remaining almost constant at about 20 mV. A small change with the shift of the midpoint potential to a more positive value is observed below pH 2.5, indicating that the redox process begins to be H^+ dependent. Taking into account that $(\equiv SiO)_2Ti(O_3POH)_2$ is a highly porous substrate, the organic molecule can be entrapped as the protonated form in the xerogel pores and, thus, the measured midpoint potential does not depend on the H^+ of the solution, in contrast to those observed for graphite/MLB (Fig. 3a). For a pH lower than 2.5 the midpoint potential starts to be dependent on the H^+ of the solution, suggesting a more protonated form for these solutions. The matrix affinity by the organic molecule is very high, and even at a higher solution pH and in the presence of a large concentration of the supporting electrolyte solution it is not released to the solution phase. Measuring the potentials in other common electrolytes, in neutral solution, no significant variation of the E_m values are observed (Table 1). Similar electrochemical behaviour was recently reported for Nile Blue and Methylene Blue entrapped in zirconium phosphate lamella [23, 24].

Table 1 Midpoint potentials of $(\equiv 0SiO)_2Ti(O_3POMLB)_2$ in various electrolyte solutions. Concentration of the electrolyte: 0.5 M, pH 6.5; scan rate: 20 mV s^{-1}

Electrolyte	E_m (V)	ΔE_p (mV)
KCl	0.023	109
K_2SO_4	0.020	102
LiCl	0.010	187
NaCl	0.020	139
NH_4Cl	0.011	97

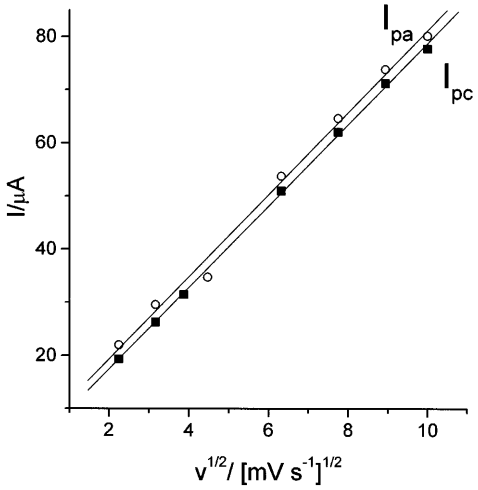

Fig. 4 Plot of the anodic (I_{pa}) and cathodic (I_{pc}) peak currents against $v^{1/2}$ in 0.5 M KCl solution at pH 6.5

A linear correlation plotting I against $v^{1/2}$ (where I = current, v = scan rate) for the immobilized MLB material was observed (Fig. 4), indicating that the redox reaction is controlled by the electrolyte diffusion into the matrix. The average pores size of the matrix are sufficiently large and, thus, cations of the supporting electrolyte can move easily into and out at the solid-solution interface in the redox process. The process is shown in below:

$$(\equiv SiO)_2Ti(O_3POMLB_{ox})_2 + 4K^+ + 4e^- \rightleftharpoons (\equiv SiO)_2Ti(O_3POMLB_{red})_2K_4 \quad (2)$$

Since the electroactive species is found entrapped in the matrix pores, the kinetic evaluation of the redox process at the electrode-solution interface is very important. By using the Laviron treatment [28] {plotting $(E_{pa}–E_m)/(E_{pc}–E_m)$ as a function of $n\Delta E_p$ (n is the number of electrons and ΔE_p is the peak separation) and E_{pa} and E_{pc} vs. log v}, the transfer coefficient (α) value was estimated as being 0.5. The k (rate constant of electron transfer) value for $v = 1$ V s^{-1} was estimated as being 16.9 s^{-1}. This value is not very high, indicating that there is some resistance to the electron transfer, but considering that the material is not totally a conductor and the electroneutrality is made by the electrolyte species, this value is reasonable.

Electrochemical oxidation of hydrazine

Studies of electrooxidation of hydrazine were made by immersing $(\equiv SiO)_2Ti(O_3POMLB)_2$ in 2×10^{-4} M hydrazine solution at different pH values to determine how the anodic peak current varies (Table 2). The best response was obtained for hydrazine solution when the pH was adjusted to about 6.

Table 2 Variation of anodic peak currents, ΔI, against the solution pH variation on hydrazine oxidation in KCl 0.5 M solution at a scan rate of 20 mV s^{-1}

ΔI (μA)	22.6	25.5	32.5	30.0
pH	4	5	6	7

Under such a condition, the dependence of the catalytic current intensities with the changes of hydrazine concentrations were shown to be linear. Plotting the anodic peak currents against hydrazine concentrations, a linear correlation was observed between 0.01 and 0.06 M (Fig. 5). The equation fit is $\Delta I_{pa} = (347 \pm 3) + (3.80 \pm 0.07)$[hydrazine], where the current is in μA and the concentration in μM, with a correlation coefficient of 0.998 for $n = 10$.

The reactions at the solid-solution interface can be represented as shown below:

$$\{(\equiv SiO)_2Ti(O_3POMLB_{red})_2K_4\} \rightleftharpoons (\equiv SiO)_2Ti(O_3POMLB_{ox})_2 + 4K^+ + 4e^- \quad (3)$$

$$(\equiv SiO)_2Ti(O_3POMLB_{ox})_2 + N_2H_4 \rightarrow [(\equiv SiO)_2Ti(O_3POMLB_{ox})_2 \ldots (N_2H_4)] \quad (4)$$

$$[(\equiv SiO)_2Ti(O_3POMLB_{ox})_2 \ldots (N_2H_4)] \rightarrow (\equiv SiO)_2Ti(O_3POMLB_{red})_2 + N_2 + H^+ \quad (5)$$

where Eq. 3 shows the electrochemical oxidation of the dye, Eq. 4 the transition state, and Eq. 5 the oxidation of the hydrazine by MLB_{ox}.

Conclusions

Meldola's Blue is immobilized very efficiently on the $(\equiv SiO)_2Ti(O_3POH)_2$ substrate. The high matrix affinity by the dye, which is incorporated as the protonated-entrapped form, is presumably the reason why the redox potential of the adsorbed dye remained almost constant between pH 3 and 7. In this case, even if the pH of the solution phase changes, i.e. it becomes higher, the strongly adsorbed dye on the solid phase will remain in the protonated form.

Owing to the high porous nature of the material, a high current density is observed for electrodes made with the material. The specific surface area is 595 $m^2\ g^{-1}$ and the amount of the adsorbed dye is 0.62 mmol g^{-1}. If we assume that the dye uniformly covers the surface, the surface density of the electroactive species is 1.0×10^{-10} mol cm^{-2} (about 1.6 molecules nm^{-2}).

The anodic potential under which the hydrazine is oxidized is low, in contrast to those observed for oxidation on a graphite electrode surface. The electrode did not show significant changes in response for a month of use, showing good chemical stability. These characteristics make the present material very attractive in using as a sensor for this analyte.

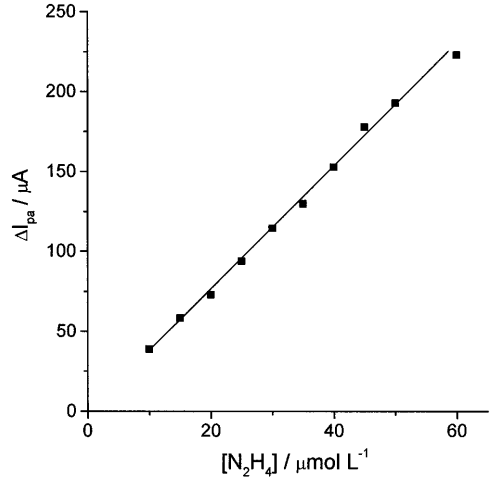

Fig. 5 Plot of the anodic peak current intensities variation (ΔI_{pa}) against hydrazine concentration. Scan rate of 20 mV s^{-1}; 0.5 M KCl; pH 6.5

Acknowledgements The authors are indebted to FAPESP for financial support and to CNPq for a fellowship to C.U.F.

References

1. Zaldivar GAP, Gushikem Y, Kubota LT (1991) J Electroanal Chem 318: 247–254
2. Kubota LT, Gushikem Y (1992) Electrochim Acta 37: 2477–2480
3. Zaldivar GAP, Gushikem Y (1992) J Electroanal Chem 337: 165–174
4. Andreotti EIS, Gushikem Y, Kubota LT (1992) J Braz Chem Soc 3: 21–24
5. Kubota LT, Gushikem Y (1993) J Electroanal Chem 362: 219–225
6. Zaldivar GAP, Gushikem Y, Benvenutti EV, de Castro SC, Vasquez A (1994) Electrochim Acta 39: 33–36
7. Peixoto CRM, Kubota LT, Gushikem Y (1995) Anal Proc 32: 503–505
8. Gushikem Y, Peixoto CRM, Rodrigues Filho UP, Kubota LT, Stadler E (1996) J Colloid Interface Sci 184: 236–240
9. Alfaya AAS, Gushikem Y(1999) J Colloid Interface Sci 209: 428–434
10. Lev O, Wu Z, Bharathi S, Glezer V, Modestov A, J Gun, L Rabinovich, Sampath S (1997) Chem Mater 9: 2354–2375
11. Hsueh CC, Collinson MM (1997) J Electroanal Chem 420: 243–249
12. Kim W, Chung S, Park SC, Lee SC, Kim C, Sung DD (1997) Anal Chem 69: 95–98
13. Li J, Chia LS, Goh NK, Tan SN (1998) Anal Chim Acta 362: 203–211
14. Li J, Tan SN, Oh JT (1998) J Electroanal Chem 448: 69–77
15. Díaz NA, Peinado MCR, Minguez MCT (1998) Anal Chim Acta 363: 221–227
16. Walcarius A (1998) Electroanalysis 10: 1217–1235
17. Alfaya AAS, Gushikem Y, de Castro SC (1998) Chem Mater 10: 909–913
18. Gorton L, Torstensson A, Jaegfeldt H, Johansson G (1984) J Electroanal Chem 161: 103–120
19. Bishop E (1972) Indicators. In: Belcher R, Frieser H (eds) International series of monographs in analytical chemistry, vol 51. Pergamon Press, Oxford
20. Persson B, Gorton L (1990) J Electroanal Chem 292: 115–138

21. Gorton L, Johansson G, Torstensson A (1985) J Electroanal Chem 196: 81–92
22. Kubota LT, Gouveia F, Andrade AN, Milagres BG, de Oliveira Neto G (1996) Eletrochim Acta 41: 1465 –1469
23. Pessoa CA, Gushikem Y, Kubota LT, Gorton L (1997) J Electroanal Chem 431: 23–27
24. Pessoa CA, Gushikem Y, Kubota LT (1997) Electronalysis 9: 800–803
25. Zagal JH, Lira S, Zañartu SU (1986) J Electroanal Chem 210: 95–110
26. Goodhew PJ, Humphreys FJ (1988) Electron microscopy and analysis, 2nd edn. Taylor and Francis, London, p 157
27. Nakayama H, Eguchi T, Nakamura N, Yamaguchi S, Danjyo M, Tsuhako M (1997) J Mater Chem 7: 1063–1066
28. Laviron E (1979) J Electroanal Chem 101: 19–28